Available online at www.sciencedirect.com
SCIENCE DIRECT®
Journal of Molecular Catalysis B: Enzymatic 22 (2003) 181–192
JOURNAL OF MOLECULAR CATALYSIS B: ENZYMATIC
www.elsevier.com/locate/molcatb

Transition-state models are useful for versatile biocatalysts: kinetics and thermodynamics of enantioselective acylations of secondary alcohols catalyzed by lipase and subtilisin

Tadashi Ema*, Kunihiro Yamaguchi, Yuji Wakasa, Akinori Yabe, Ryoichi Okada, Minoru Fukumoto, Fumika Yano, Toshinobu Korenaga, Masanori Utaka, Takashi Sakai[1]

Department of Applied Chemistry, Faculty of Engineering, Okayama University, Tsushima, Okayama 700-8530, Japan

Received 24 December 2002; received in revised form 12 February 2003; accepted 24 February 2003

Abstract

Lipases and subtilisins are versatile enzymes capable of showing high enantioselectivity and broad substrate specificity simultaneously. The transition-state models previously proposed to rationalize this important feature were intensively examined from kinetic and thermodynamic viewpoints. Kinetic measurements reaffirmed that chiral discrimination originates from the transition state and that the enantioselectivity results from the reduced activity of the enzymes for the slower-reacting enantiomer, but not from the enhanced activity for the faster-reacting enantiomer relative to a reference alcohol, cyclopentanol. The larger substituent of the slower-reacting enantiomers interacts repulsively with the protein in the transition state, and even the larger substituent of the faster-reacting enantiomers interacts unfavorably to some degree with the protein. A number of thermodynamic parameters, $\Delta\Delta H^{\ddagger}$ and $\Delta\Delta S^{\ddagger}$, for the subtilisin-catalyzed acylations of secondary alcohols were determined. A linear compensation effect was found between the $\Delta\Delta H^{\ddagger}$ and $\Delta\Delta S^{\ddagger}$ values. As the $\Delta\Delta H^{\ddagger}$ value becomes negatively large, the $\Delta\Delta S^{\ddagger}$ value also becomes negatively large. This observation is explained in terms of the transition-state model. Because the widely accepted concepts such as the lock-and-key mechanism and the induced-fit mechanism cannot account for the peculiar behavior of these enzymes toward unnatural substrates, a new category, the non-lock-and-key mechanism, has been proposed.

Keywords: Lipase; Subtilisin; Enantioselectivity; Mechanism

1. Introduction

Lipases are currently one of the best biocatalysts for the preparation of a wide range of optically active secondary alcohols [1–6]. They show high enantioselectivity and broad substrate specificity simultaneously. Uncovering the origin of this unique feature of lipases is an important subject. Several methods have been used to disclose the mechanism of enantioselectivity: (i) substrate mapping [7–16], (ii) X-ray crystallographic analysis [17–20], (iii) computational calculations [21–27], (iv) kinetic analysis [28–31], (v) thermodynamic analysis [32–34], (vi) site-directed or

* Corresponding author. Tel.: +81-86-251-8091; fax: +81-86-251-8092.
E-mail address: ema@cc.okayama-u.ac.jp (T. Ema).
[1] Co-corresponding author.

1381-1177/03/$ – see front matter © 2003 Elsevier Science B.V. All rights reserved.
doi:10.1016/S1381-1177(03)00034-1

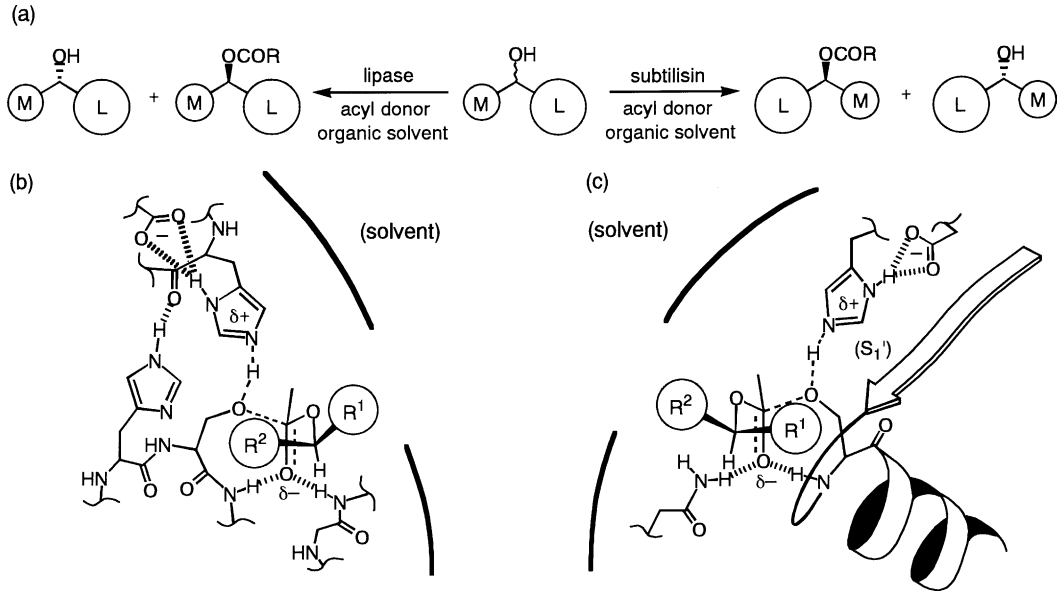

Fig. 1. (a) Empirical rules for the lipase- and subtilisin-catalyzed kinetic resolutions of secondary alcohols. L and M represent the larger and smaller substituents, respectively. Typically, (*R*)- and (*S*)-enantiomers react faster in the lipase- and subtilisin-catalyzed kinetic resolutions, respectively. (b and c) Transition-state models for the (b) lipase- and (c) subtilisin-catalyzed kinetic resolutions of secondary alcohols. In both models, (i) the C–O bond of a substrate takes the *gauche* conformation with respect to the breaking C–O bond, which is due to the stereoelectronic effect, and (ii) the H atom attached to the asymmetric C atom of the substrate is *syn*-oriented toward the carbonyl O atom of the acetyl group. When such a locally favorable conformation is taken, the faster-reacting enantiomer can direct the larger substituent (R^1 in (b) and R^2 in (c)) toward external solvent without severe steric hindrance, whereas the slower-reacting enantiomer directs the larger substituent (R^2 in (b) and R^1 in (c)) toward the protein wall, causing a severe steric repulsion. Even if any other conformation is taken, the slower-reacting enantiomer necessarily becomes less stable than the antipodal enantiomer. For details, see [42].

random mutagenesis [35–40], and (vii) mass spectroscopy [41]. Because any of the methods has merits and demerits, the validity of a proposed mechanism should always be examined and evaluated by using different methods.

Previously, we have proposed a stereo-sensing mechanism of lipases (Fig. 1b) [42]. In this model, enantioselectivity is explained only by the conformational requirements and repulsive interactions in the transition state, and no binding interaction between enzyme's pockets and substrate's substituents is involved. In this sense, lipases are considered to be "chemical reagent-like" [43]. Further studies have indicated that such a concept can be applied to subtilisins (Fig. 1c) [44]. These transition-state models can rationalize (i) the simultaneous achievement of high enantioselectivity and broad substrate specificity, (ii) the opposite enantiopreferences of lipases [7–16] and subtilisins [44–47] for secondary alcohols (Fig. 1a), (iii) low activity for secondary alcohols having bulky substituents on both sides [42], (iv) little or no activity for tertiary alcohols [42], and other experimental observations. These transition-state models have been derived on the basis of molecular orbital calculations and molecular modeling [42] and have been supported by the kinetic [42,44] and thermodynamic [48] studies. The local conformation shown in the transition-state models has been experimentally supported by using an extremely large secondary alcohol, 5-[4-(1-hydroxyethyl)phenyl]-10,15,20-triphenylporphyrin, as a substrate [44,49,50].

Among several methods listed above, kinetic and thermodynamic analysis as well as substrate mapping can rapidly provide fundamental and useful data for elucidating the origin of enantioselectivity. We therefore employed these methods to examine further the validity of the transition-state models shown in Fig. 1b and c. The preliminary papers have been reported

elsewhere [44,48]. Although lipases and subtilisins are entirely different kinds of enzymes, we present the results for both enzymes together in this paper to demonstrate the validity of the common mechanism represented by Fig. 1. We also propose a new term, the "non-lock-and-key mechanism", to represent a new category of enantioselective enzymatic reactions because the traditional lock-and-key paradigm cannot account for the unusual behavior of these synthetically useful enzymes toward unnatural substrates.

2. Experimental

2.1. General

^{1}H NMR spectra were measured in $CDCl_3$ at 200 MHz. Thin layer chromatography (TLC) was performed on Merck silica gel 60 F_{254}. Silica gel column chromatography was performed using Fuji Silysia BW-127 ZH (100–270 mesh). Lipase PS was a gift from Amano Enzyme Inc., and ChiroCLEC-BL was purchased from Altus Biologics Inc. Dry *i*-Pr_2O was distilled from sodium. Substrates **1**–**11** are commercially available. Enantiomerically pure alcohols (>99% ee) were prepared by the lipase-catalyzed kinetic resolutions of racemic alcohols according to the previously reported procedure [42]. The kinetic measurements for the lipase-catalyzed reactions were performed as described previously [42]. The reaction conditions for the PCL- and SC-catalyzed kinetic resolutions of **12** have been reported in [50].

2.2. Determination of enantiomeric purity

The enantiomeric purities of alcohols **1**, **5**, and **8**–**11** were determined without derivatization. All the other alcohols were converted to the corresponding acetates. The enantiomeric purities of **1**–**5** and **7** were determined by capillary GC using a CP-cyclodextrin-β-2,3,6-M-19 column (Chrompack, ϕ 0.25 mm × 25 m). GC for **1**: Inj. 250 °C, Col. 100 °C, Det. 220 °C, (*R*) 22 min, (*S*) 25 min. GC for **1** (acetate form): Inj. 250 °C, Col. 100 °C, Det. 220 °C, (*S*) 20 min, (*R*) 22 min. GC for **2** (acetate form): Inj. 250 °C, Col. 100 °C, Det. 220 °C, (*S*) 18 min, (*R*) 20 min. GC for **3** (acetate form): Inj. 300 °C, Col. 100 °C, Det. 220 °C, (*S*) 30 min, (*R*) 33 min. GC for **4** (acetate form): Inj. 300 °C, Col. 110 °C, Det. 220 °C, (*S*) 40 min, (*R*) 45 min. GC for **5**: Inj. 250 °C, Col. 100 °C, Det. 220 °C, (*R*) 16 min, (*S*) 18 min. GC for **7** (acetate form): Inj. 250 °C, Col. 80 °C, Det. 220 °C, (*S*) 11 min, (*R*) 14 min. The enantiomeric purities of **6** and **8**–**11** were determined by HPLC using chiral columns (Daicel Chemical Industries). HPLC for **6** (acetate form): Chiralpak AD, hexane/*i*-PrOH = 100:1, flow rate 0.5 ml/min, detection 254 nm, (*S*) 12 min, (*R*) 13 min. HPLC for **8**: Chiralcel OD-H, hexane/*i*-PrOH = 100:1, flow rate 1.0 ml/min, detection 260 nm, (*S*) 17 min, (*R*) 19 min. HPLC for **9**: Chiralcel OB-H, hexane/*i*-PrOH = 9:1, flow rate 0.5 ml/min, detection 254 nm, (*R*) 13 min, (*S*) 18 min. HPLC for **10**: Chiralcel OB-H, hexane/*i*-PrOH = 9:1, flow rate 0.5 ml/min, detection 254 nm, (*S*) 24 min, (*R*) 27 min. HPLC for **11**: Chiralcel OB-H, hexane/*i*-PrOH = 9:1, flow rate 0.5 ml/min, detection 254 nm, (*R*) 29 min, (*S*) 33 min.

2.3. Kinetic measurements for subtilisin-catalyzed reactions

A stock solution of 5.0 M vinyl acetate in dry *i*-Pr_2O was prepared beforehand. A heterogeneous solution of (enantiomerically pure) alcohol (typically, 5–60 mM), ChiroCLEC-BL (typically, 20 mg for (*R*)-enantiomer and 3–10 mg for (*S*)-enantiomer), and MS 4A (80 mg) in dry *i*-Pr_2O (3.6 ml) in a test tube with a rubber stopper was stirred at 450 rpm in a water bath thermostated at 30 °C. After 5 min, the stock solution of vinyl acetate (0.40 ml) was added to the heterogeneous solution to start the reaction (0.50 M vinyl acetate). At an appropriate time interval, aliquots (50–100 μl) were withdrawn and centrifuged at 6400 rpm for 30 s. The supernatant was analyzed by GC to obtain the conversion, c (c < 15%, calibrated). Five data points were routinely collected to determine the initial rate (ν_0) at each substrate concentration $[S]_0$. Plot of ν_0 against $[S]_0$ afforded a saturation curve, and the apparent V_{max} and K_m values were obtained by the nonlinear least-squares method applied to the Michaelis–Menten type of equation: $\nu_0 = V_{max}(E)_{mg}[S]_0/(K_m + [S]_0)$, where V_{max} is normalized by the weight of the lipase $(E)_{mg}$ because of the heterogeneous system.

2.4. Thermodynamic measurements for subtilisin-catalyzed kinetic resolutions

A mixture of alcohol (0.82 mmol), ChiroCLEC-BL (40 mg) and MS 4A (400 mg) in dry *i*-Pr_2O (5 ml) in a test tube with a rubber septum was stirred for 23 h in a water bath thermostated at 30 °C. After the mixture was stirred for 1 h at the reaction temperature (10, 20, 30, or 40 °C), vinyl acetate (141 mg, 1.64 mmol) was added. The progress of the reaction was monitored by TLC. The reaction was stopped by filtration through Celite, and the filtrate was concentrated under reduced pressure. Alcohol and acetate were separated by silica gel column chromatography and analyzed by HPLC or GC to determine the enantiomeric purities. The *E* values were calculated according to the literature [51]. The *E* values were measured at several reaction temperatures, and the thermodynamic parameters were calculated according to Eq. (1) shown later.

2.5. Thermodynamic measurements for lipase-catalyzed kinetic resolutions

Because we observed that a small amount of water or moisture can affect the *E* value, slight differences in experimental conditions may lead to different thermodynamic parameters. A mixture of alcohol (0.82 mmol) and lipase PS (270 mg) in dry *i*-Pr_2O (5 ml) in a test tube with a rubber septum was stirred for 30 min in a water bath thermostated at the reaction temperature (20, 30, 40, 50, or 60 °C). The reaction was started by adding vinyl acetate (141 mg, 1.64 mmol). The subsequent procedure was done as described above.

3. Results and discussion

3.1. Substrate mapping

Pseudomonas cepacia lipase (PCL, lipase PS) and subtilisin Carlsberg (SC, ChiroCLEC-BL) were employed as biocatalysts. The PCL- and SC-catalyzed kinetic resolutions of secondary alcohols **1**–**11** (Scheme 1) were performed with vinyl acetate in dry *i*-Pr_2O at 30 °C. In the case of the SC-catalyzed reactions, molecular sieves (MS) 4A was added to improve the apparent reaction rates, which was probably due to removal of water from the cross-linked enzyme crystals. The results are shown in Table 1. The *E* values for **12** are taken from the literature [49,50].

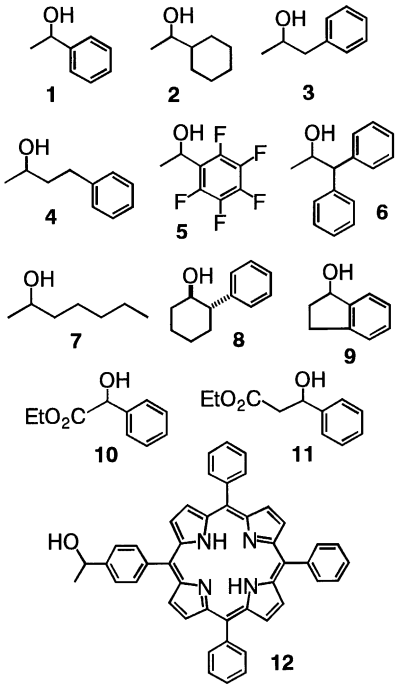

Scheme 1.

PCL and SC exhibited the opposite enantiopreferences for **1**–**5**, **7**–**9**, and **12**. Because an approximate mirror-image relationship exists between the catalytic residues (the catalytic triad and the oxyanion hole) of lipases and those of the serine proteases [52], the opposite enantiopreferences of PCL and SC can be rationalized by the transition-state models using the local conformational requirements and repulsive interactions (Fig. 1b and c). In contrast, it is difficult to ascribe the opposite enantiopreferences to binding interactions between enzyme's pockets and substrate's substituents because the potential binding pockets of PCL and SC do not appear to be disposed in a mirror-image fashion. From practical viewpoints, an impure lipase preparation that contains serine protease (vice versa) should be avoided particularly for the purpose of kinetic resolution of secondary alcohols, because the enantioselectivity will be decreased by their opposite enantiopreferences.

Table 1
PCL- and SC-catalyzed kinetic resolutions of **1**–**12** in *i*-Pr_2O at 30 °C[a]

Alcohol	PCL		SC	
	E value	*R*/*S*[b]	*E* value	*R*/*S*[b]
1	>317	*R*	10	*S*
2	138	*R*	8	*S*
3	>331	*R*	40	*S*
4	>307	*R*	28	*S*
5	>307	*R*	59	*S*
6	–[c]	–	6	*S*
7	13	*R*	13	*S*
8	>321	*R*	28	*S*
9	340	*R*	3	*S*
10	66	*S*	7	*S*
11	9	*R*	2	*R*
12	>298[d]	*R*	140[e]	*S*

[a] For detailed reaction conditions, see Section 2.
[b] Enantiopreference.
[c] No reaction.
[d] Data taken from [49].
[e] Data taken from [50].

There is a clear tendency that the *E* values for the SC-catalyzed reactions are much lower than those for the corresponding PCL-catalyzed reactions (Table 1). This reduced enantioselectivity of SC is probably due to the lack of a protein wall. PCL has the "triangular wall" (Fig. 1b) that has been proposed to be important for enantiomer discrimination [42], whereas SC has the shallow depression (S_1') that is made up of the β-strand, the α-helical turn, and the histidine imidazole of the catalytic triad (Fig. 1c) [53–55]. Owing to this S_1' depression, the steric repulsion point in SC is distant from the stereocenter of the secondary alcohol in the transition state as compared to the case of PCL. Visual inspection of the crystal structure of SC suggested that this space is as large as a benzene ring. SC may therefore have poor ability to discriminate the chirality of **1**, **2**, and **9**–**11**.

Table 1 exhibits another trend for the SC-catalyzed reactions: as the bulkiness of the two substituents is unbalanced, the enantioselectivity is higher. For example, the *E* values increase in the order of **1**, **3**, **5**, and **12**. The transition-state model suggests that one substituent is directed toward the protein and that the other substituent is directed toward external solvent. Therefore, as the bulkiness of the two substituents is unbalanced, the difference in the steric repulsion caused in the transition state between the enantiomers becomes large, leading to higher enantioselectivity. In the case of **10** and **11** having bulky substituents on both sides, however, it is difficult to judge unambiguously which of the two substituents is more bulky. Actually, PCL and SC exhibited the same enantiopreference for **10** and **11**, suggesting that PCL disfavors the phenyl group rather than the ethoxycarbonyl group, while SC disfavors the ethoxycarbonyl group rather than the phenyl group. The transition-state model may be too simple to explain the low *E* value for **6** in comparison to that for **3**. Factors that are not shown in Fig. 1c may also be important for **6**. The result that PCL showed no activity for **6** suggests that even (*R*)-**6** cannot approach the active site because of a steric repulsion between the diphenyl moiety of (*R*)-**6** and a protein moiety that is not shown in the transition-state model (Fig. 1b).

3.2. Kinetic study

Kinetic analysis can clearly reveal the enantiomer-discriminating step and the relative stability of the enantiomers in distinct steps. The enantiomerically pure alcohols **1**–**5** and **8** were prepared according to the reported procedure [42]. The kinetic measurements for the enzyme-catalyzed transesterifications were performed with 0.5 M vinyl acetate in dry *i*-Pr_2O at 30 °C in the presence of MS 4A. The kinetic parameters, V_{max} and K_m, for enantiomerically pure alcohols, cyclopentanol, and cyclohexanol were determined by fitting the data to the Michaelis–Menten type of equation, $v_0 = V_{max}(E)_{mg}[S]_0/(K_m + [S]_0)$, as reported previously [42]. It is known that a caution is necessary for approximation of $K_m = (k_{-1} + k_{cat})/k_1$; when k_{cat} is comparable to k_{-1}, K_m cannot be equal to K_s, the dissociation constant (Briggs–Haldane kinetics) [56]. This is known to hold for some efficient enzymatic reactions toward physiological substrates [56]. In our case, however, because of the reactions toward unnatural substrates, secondary alcohols, and because of the enzymatic reactions in an organic solvent, k_{cat} is considered to be much smaller than k_{-1}, which allows us to take K_m as K_s approximately (Michaelis–Menten kinetics). We neglected the contribution of non-productive binding because non-productive binding does not alter the specificity constant, k_{cat}/K_m, and hence enantioselectivity [56],

Table 2
Kinetic parameters for PCL-catalyzed transesterifications of secondary alcohols[a]

Alcohol	V_{max} (M min^{-1} mg (enzyme)$^{-1}$)		K_m (M)	
	R	*S*	*R*	*S*
1[b]	$(3.7 \pm 0.4) \times 10^{-5}$	$(6.6 \pm 0.9) \times 10^{-8}$	$(1.0 \pm 0.2) \times 10^{-1}$	$(9.9 \pm 3.8) \times 10^{-2}$
2[b]	$(3.4 \pm 0.1) \times 10^{-5}$	$(3.1 \pm 0.4) \times 10^{-7}$	$(1.4 \pm 0.1) \times 10^{-1}$	$(2.6 \pm 0.6) \times 10^{-1}$
3[b]	$(1.3 \pm 0.2) \times 10^{-5}$	$(3.2 \pm 0.7) \times 10^{-8}$	$(1.4 \pm 0.4) \times 10^{-1}$	$(4.6 \pm 1.6) \times 10^{-1}$
4	$(9.2 \pm 0.2) \times 10^{-6}$	$(1.0 \pm 0.1) \times 10^{-8}$	$(1.7 \pm 0.1) \times 10^{-1}$	$(5.1 \pm 1.3) \times 10^{-2}$
5	$(1.4 \pm 0.7) \times 10^{-6}$	–[c]	1.2 ± 0.9	–[c]
8	$(2.1 \pm 0.2) \times 10^{-6}$	–[c]	$(9.2 \pm 1.8) \times 10^{-2}$	–[c]
Cyclopentanol[b]	$(1.4 \pm 0.1) \times 10^{-4}$		$(1.7 \pm 0.2) \times 10^{-1}$	
Cyclohexanol	$(4.7 \pm 0.8) \times 10^{-5}$		$(1.8 \pm 0.5) \times 10^{-1}$	

[a] Conditions: lipase PS (typically, 20–300 and 300 mg for the (*R*)- and (*S*)-enantiomers, respectively), alcohol (typically, ca. 0.02–0.3 M), vinyl acetate (0.50 M), three pieces of MS 4A, dry *i*-Pr_2O (2.0 ml), 30 °C. Because of the heterogeneous reaction, the nonlinear least-squares method was applied to the Michaelis–Menten type of equation: $v_0 = V_{max}(E)_{mg}[S]_0/(K_m + [S]_0)$, where V_{max} is normalized by the weight of the enzyme $(E)_{mg}$.

[b] Data taken from [42].

[c] No reaction even in the presence of a large amount (300 mg) of lipase PS.

and because very large K_m values, as shown below, strongly suggested very weak binding. The V_{max} value, which is normalized by the weight of the enzyme powder $(E)_{mg}$, corresponds to the k_{cat} value in homogeneous enzymatic reactions, but the V_{max} value cannot be compared among different enzymes because the enzyme preparations contain a different amount of supporting material. Despite some ambiguity in steady-state kinetics, we used the V_{max} and K_m values separately to estimate the relative stability of distinct steps. Although 2-propanol can serve as an ideal reference standard for **1**–**5**, attempts to separate the GC peak of 2-propanol from the solvent peak were unsuccessful. Cyclopentanol was therefore used as a reference alcohol for all the chiral secondary alcohols. For more accurate comparisons, cyclohexanol can be used as a reference alcohol for **8**. The results are listed in Tables 2 and 3.

Tables 2 and 3 clearly show the following significant points: (i) the difference in the V_{max} value between the enantiomers is much larger than that in the K_m value between the enantiomers, which indicates that chiral discrimination originates from the transition state, but not from the substrate-binding step, and

Table 3
Kinetic parameters for SC-catalyzed transesterifications of secondary alcohols[a]

Alcohol	V_{max} (M min^{-1} mg (enzyme)$^{-1}$)		K_m (M)	
	R	*S*	*R*	*S*
1	$(1.1 \pm 0.2) \times 10^{-5}$	$(1.1 \pm 0.2) \times 10^{-4}$	$(2.2 \pm 0.8) \times 10^{-2}$	$(2.0 \pm 0.7) \times 10^{-2}$
2	$(2.2 \pm 0.1) \times 10^{-6}$	$(3.6 \pm 0.4) \times 10^{-5}$	$(1.6 \pm 0.2) \times 10^{-1}$	$(2.2 \pm 0.5) \times 10^{-1}$
3	$(5.3 \pm 0.2) \times 10^{-7}$	$(6.1 \pm 0.3) \times 10^{-5}$	$(1.7 \pm 0.1) \times 10^{-2}$	$(1.7 \pm 0.2) \times 10^{-2}$
4	$(8.5 \pm 1.2) \times 10^{-7}$	$(3.5 \pm 0.5) \times 10^{-5}$	$(3.7 \pm 1.0) \times 10^{-2}$	$(1.7 \pm 0.6) \times 10^{-2}$
5	$(1.1 \pm 0.3) \times 10^{-7}$	$(5.0 \pm 0.2) \times 10^{-6}$	$(6.8 \pm 2.6) \times 10^{-2}$	$(1.3 \pm 0.1) \times 10^{-2}$
8	$(5.4 \pm 0.7) \times 10^{-8}$	$(5.4 \pm 0.1) \times 10^{-6}$	$(2.2 \pm 0.9) \times 10^{-2}$	$(2.5 \pm 0.1) \times 10^{-2}$
Cyclopentanol	$(2.2 \pm 0.1) \times 10^{-4}$		$(1.5 \pm 0.2) \times 10^{-1}$	
Cyclohexanol	$(5.7 \pm 0.5) \times 10^{-5}$		$(2.9 \pm 0.9) \times 10^{-2}$	

[a] Conditions: ChiroCLEC-BL (typically, 20 and 3–10 mg for the (*R*)- and (*S*)-enantiomers, respectively), alcohol (typically, ca. 0.005–0.06 M), vinyl acetate (0.50 M), MS 4A (80 mg), dry *i*-Pr_2O (4.0 ml), 30 °C. Because of the heterogeneous reaction, the nonlinear least-squares method was applied to the Michaelis–Menten type of equation: $v_0 = V_{max}(E)_{mg}[S]_0/(K_m + [S]_0)$, where V_{max} is normalized by the weight of the enzyme $(E)_{mg}$.

(ii) the V_{max} values for the faster- and slower-reacting enantiomers are somewhat smaller and considerably smaller, respectively, than those for the reference alcohols, indicating that the enantioselectivity results from the greatly reduced activity of the enzymes for the slower-reacting enantiomers, but not from the enhanced activity for the faster-reacting enantiomers. Clearly, the larger substituent of the slower-reacting enantiomers interacts repulsively with the protein in the transition state, and even the larger substituent of the faster-reacting enantiomers interacts unfavorably with the protein. Although this conclusion holds for both enzymes, PCL has a stronger tendency to hinder the reaction of the slower-reacting enantiomers as compared to SC, which accounts for the higher enantioselectivity of PCL as compared to SC (Table 1).

To see the poor binding capacity of the enzymes, the binding energies (ΔG°) and the differential binding energies ($\Delta\Delta G^\circ$) were estimated from $RT\ln K_m$ and were then compared with the chiral discrimination energies ($\Delta\Delta G^\ddagger$) calculated from $-RT\ln E$. The values are listed in Table 4. The ΔG° values are relatively large, ranging from $+0.1$ to $-1.8\,\mathrm{kcal\,mol^{-1}}$ for PCL and from -0.9 to $-2.6\,\mathrm{kcal\,mol^{-1}}$ for SC. The $\Delta\Delta G^\circ$ values, ranging from $+0.7$ to $-0.7\,\mathrm{kcal\,mol^{-1}}$ for PCL and from $+0.2$ to $-1.0\,\mathrm{kcal\,mol^{-1}}$ for SC, are trifling as compared to the $\Delta\Delta G^\ddagger$ values, ranging from -3.0 to $<-3.5\,\mathrm{kcal\,mol^{-1}}$ for PCL and from -1.3 to $-2.5\,\mathrm{kcal\,mol^{-1}}$ for SC. Thus, the binding capacity (ΔG°) and the chiral recognition ability ($\Delta\Delta G^\circ$) of PCL are too poor to drive the high degree of enantiomer discrimination ($\Delta\Delta G^\ddagger$). Although, in the case of the SC-catalyzed reactions, the ΔG° values are comparable to the $\Delta\Delta G^\ddagger$ values, it is difficult to attribute the good enantioselectivity ($\Delta\Delta G^\ddagger$) to the low chiral recognition ability ($\Delta\Delta G^\circ$).

There are no indications, not only in the substrate-binding step but also in the transition state, that the faster-reacting enantiomers are stabler than the reference alcohol. Tables 2 and 3 indicate that, in the transition state, even the faster-reacting enantiomers are destabilized to some extent as compared to the reference alcohol. Taken all together, we conclude that binding interactions are not important at all for enantioselectivity. This conclusion, which may appear unusual for enzymatic reactions, is quite reasonable, because it is unlikely that the enzymes have binding pockets to recognize unnatural substrates that have nothing to do with evolutionary pressure, and because it is also unlikely that hydrophobic interactions work well in organic solvents [57]; the substrate, solvated well by organic solvent molecules, must be desolvated in entering the active site of the enzyme, which is not advantageous. It should also be noted that many mechanisms proposed by other researchers, explaining the enantioselectivity by using binding interactions between enzyme's pockets and substrate's substituents, are inconsistent with these kinetic data.

Table 4
Binding energies and chiral discrimination energies at 30 °C

Enzyme	Alcohol	ΔG° (*R*)[a] (kcal mol^{-1})	ΔG° (*S*)[a] (kcal mol^{-1})	$\Delta\Delta G^\circ$[b] (kcal mol^{-1})	$\Delta\Delta G^\ddagger$[c] (kcal mol^{-1})
PCL	**1**	−1.4	−1.4	0.0	<−3.5
PCL	**2**	−1.2	−0.8	−0.4	−3.0
PCL	**3**	−1.2	−0.5	−0.7	<−3.5
PCL	**4**	−1.1	−1.8	+0.7	<−3.4
PCL	**5**	+0.1	–[d]	–[d]	<−3.4
PCL	**8**	−1.4	–[d]	–[d]	<−3.5
SC	**1**	−2.3	−2.4	−0.1	−1.4
SC	**2**	−1.1	−0.9	+0.2	−1.3
SC	**3**	−2.5	−2.5	0.0	−2.2
SC	**4**	−2.0	−2.5	−0.5	−2.0
SC	**5**	−1.6	−2.6	−1.0	−2.5
SC	**8**	−2.3	−2.2	+0.1	−2.0

[a] Calculated from $RT\ln K_m$.
[b] Calculated from ΔG° (*R*) − ΔG° (*S*) for PCL and from ΔG° (*S*) − ΔG° (*R*) for SC.
[c] Calculated from $-RT\ln E$.
[d] No reaction.

3.3. Thermodynamic study

Since the low to moderate enantioselectivity of SC for a variety of alcohols (Table 1) enabled us to determine the reliable E values at a range of temperatures, the thermodynamic parameters for SC were first determined. The $\Delta\Delta H^{\ddagger}$ and $\Delta\Delta S^{\ddagger}$ values were determined according to Eq. (1), where $\Delta\Delta H^{\ddagger} = \Delta H^{\ddagger}_{\text{fast}} - \Delta H^{\ddagger}_{\text{slow}}$ and $\Delta\Delta S^{\ddagger} = \Delta S^{\ddagger}_{\text{fast}} - \Delta S^{\ddagger}_{\text{slow}}$ [58–60]. The thermodynamic parameters determined are listed in Table 5, together with the differential activation energies ($\Delta\Delta G^{\ddagger}$) calculated from $\Delta\Delta H^{\ddagger} - T\Delta\Delta S^{\ddagger}$. The data for **12** are taken from the literature [50].

$$\ln E = \frac{-\Delta\Delta H^{\ddagger}}{RT} + \frac{\Delta\Delta S^{\ddagger}}{R} \quad (1)$$

There is a tendency that the E value decreases with increasing temperature (data not shown). In all cases except **1**, **2**, and **9**, the $\Delta\Delta H^{\ddagger}$ value contributes predominantly to the $\Delta\Delta G^{\ddagger}$ value (Table 5), indicating that enantiomer discrimination is enthalpy-driven. There is also a tendency that the $\Delta\Delta H^{\ddagger}$ value decreases as the two substituents of the secondary alcohols are more unbalanced in bulkiness. In terms of the transition-state models, the $\Delta\Delta H^{\ddagger}$ value can be regarded as the difference in the degree of repulsive interactions with the enzyme between the enantiomers.

Table 5
Thermodynamic parameters for SC-catalyzed kinetic resolutions of **1**–**12** in *i*-Pr_2O[a]

Alcohol	$\Delta\Delta H^{\ddagger}$ (kcal mol^{-1})	$\Delta\Delta S^{\ddagger}$ (cal K^{-1} mol^{-1})	$\Delta\Delta G^{\ddagger}$[b] (kcal mol^{-1})
1	−0.21 ± 0.33	+4.0 ± 1.1	−1.4
2	−0.50 ± 0.30	+2.4 ± 1.0	−1.2
3	−3.0 ± 0.5	−2.4 ± 1.7	−2.3
4	−3.9 ± 0.3	−6.2 ± 0.9	−2.0
5	−5.2 ± 0.6	−9.3 ± 2.1	−2.4
6	−2.9 ± 0.4	−6.0 ± 1.4	−1.1
7	−1.5 ± 0.1	+0.32 ± 0.44	−1.6
8	−6.3 ± 1.3	−14 ± 4	−2.1
9	−0.10 ± 0.18	+1.7 ± 0.6	−0.6
10	−2.4 ± 0.6	−4.2 ± 2.1	−1.1
11	−1.2 ± 0.5	−2.1 ± 1.7	−0.6
12[c]	−6.8 ± 0.8	−13 ± 3	−2.9

[a] Determined by applying the least-squares method to Eq. (1).
[b] Calculated from $\Delta\Delta G^{\ddagger} = \Delta\Delta H^{\ddagger} - 303\Delta\Delta S^{\ddagger}$.
[c] Data taken from [50].

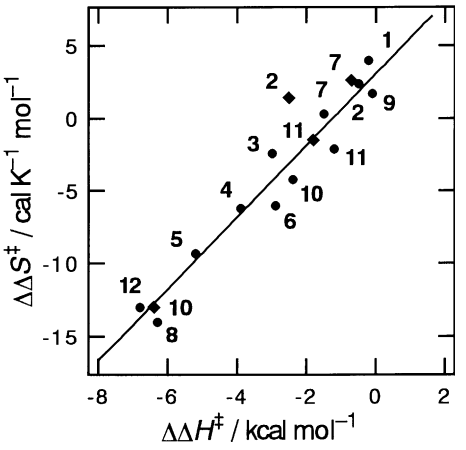

Fig. 2. Correlation plot for the $\Delta\Delta H^{\ddagger}$ and $\Delta\Delta S^{\ddagger}$ values. The data for SC- and PCL-catalyzed kinetic resolutions are shown by circles and squares, respectively. The data for **12** is taken from [50]. The line is drawn with respect to all data for SC.

Therefore, that tendency observed for the $\Delta\Delta H^{\ddagger}$ values is reasonable because the difference in the degree of repulsive interactions between the enantiomers will increase as the two substituents of the secondary alcohols are more unbalanced in bulkiness.

Interestingly, a linear relationship was found between the $\Delta\Delta H^{\ddagger}$ and $\Delta\Delta S^{\ddagger}$ values for **1**–**12** (Fig. 2). As the $\Delta\Delta H^{\ddagger}$ value becomes negatively large, the $\Delta\Delta S^{\ddagger}$ value also becomes negatively large. Similar linear relationships between the $\Delta\Delta H^{\ddagger}$ and $\Delta\Delta S^{\ddagger}$ values have been observed for diastereomeric complexation between an optically active crown ether and a variety of amines and for asymmetric photochemical reactions using optically active photosensitizers [61,62]. Eq. (1) indicates that a negative $\Delta\Delta H^{\ddagger}$ value contributes to an increase in the E value, whereas a negative $\Delta\Delta S^{\ddagger}$ value contributes to a decrease in the E value. This partial compensation effect can be understood by considering repulsive interactions between the slower-reacting enantiomer and the enzyme. In general, although repulsive interactions are unfavorable in terms of enthalpy, they are favorable in terms of entropy because the degree of disorder (or freedom) increases. Because the degree of the disorder of the amino acid residues and the substrate moiety will increase with an increase in the degree of repulsive interactions, the entropy gain will increase

Table 6
Thermodynamic parameters for PCL-catalyzed kinetic resolutions in *i*-Pr_2O[a]

Alcohol	$\Delta\Delta H^{\ddagger}$ (kcal mol^{-1})	$\Delta\Delta S^{\ddagger}$ (cal K^{-1} mol^{-1})	$\Delta\Delta G^{\ddagger}$[b] (kcal mol^{-1})
2	−2.5 ± 0.8	+1.4 ± 2.6	−2.9
7	−0.74 ± 0.15	+2.6 ± 0.5	−1.5
10	−6.4 ± 0.7	−13 ± 2	−2.5
11	−1.8 ± 1.0	−1.5 ± 3.1	−1.3

[a] Determined by applying the least-squares method to Eq. (1).
[b] Calculated from $\Delta\Delta G^{\ddagger} = \Delta\Delta H^{\ddagger} - 303\Delta\Delta S^{\ddagger}$.

proportionally with an increase in enthalpy loss. This opposite but proportional relationship between enthalpy and entropy can remain even after the $\Delta H^{\ddagger}$ and $\Delta S^{\ddagger}$ values for the slower-reacting enantiomer are subtracted from the corresponding values for the faster-reacting enantiomer. Thus, the entropic behavior can be partially explained by the enthalpic event.

As for the PCL-catalyzed kinetic resolutions of **1**, **3**–**5**, **8**, **9**, and **12**, the *E* values were too high to determine the thermodynamic parameters (Table 1). The transition-state model (Fig. 1b) suggests that the slower-reacting enantiomers of them cannot get over the transition state at all because of very high activation energies. The $\Delta\Delta H^{\ddagger}$ and $\Delta\Delta S^{\ddagger}$ values for the PCL-catalyzed kinetic resolutions of **2**, **7**, **10**, and **11** were determined, and the results are shown in Table 6. Lipases are known to take open, closed, and intermediate conformations [63]. If the lid conformation is changed with temperature, Eq. (1) cannot be valid because it is based on the assumption that the transition-state structure is kept constant over the reaction temperatures. We therefore assume that the effect of the lid on the enantioselectivity is unchanged with temperature. As observed for SC, enantiomer discrimination is enthalpy-driven, and there is a linear relationship between the $\Delta\Delta H^{\ddagger}$ and $\Delta\Delta S^{\ddagger}$ values (Fig. 2).

3.4. Non-lock-and-key concept

Owing to their extreme significance in life-sustaining enzymatic processes, the lock-and-key and induced-fit mechanisms [64–66], which are based on binding interactions, have been widely believed to operate in enzymatic reactions even toward unnatural substrates. However, these concepts cannot account for the unusual behavior of lipases and subtilisins [42,44,48–50], capable of showing high enantioselectivity and broad substrate specificity simultaneously. In this paper, no sign indicating a complementary relationship like a lock and its key could be found as a mechanistic origin of enantioselectivity. Binding is very weak, and both enantiomers are destabilized more or less as compared to the reference. Fisher's original lock-and-key hypothesis [64] and common sense nowadays [65] for explaining stereoselectivity are based on the idea that attractive interactions work between an enzyme and a favored isomer having complementary shapes to increase affinity and catalytic efficiency, whereas steric repulsions are implicitly assumed for a disfavored isomer. We agree that the lock-and-key and induced-fit mechanisms work in enzymatic reactions toward their physiological substrates. They are, however, not universal. The principle of enantioselectivity of lipases and subtilisins toward unnatural substrates, involving no binding interactions as revealed by our studies, is rather similar to that of organic reagents and cannot be classified into the lock-and-key category. A new category that differs from the traditional lock-and-key paradigm is therefore necessary for these versatile biocatalysts. We propose a new term representing the third category, the "non-lock-and-key mechanism".

Simplified energy diagrams for the lock-and-key mechanism and the non-lock-and-key mechanism are drawn in Fig. 3. In an extreme case of the lock-and-key mechanism, chiral discrimination is driven by preferential binding of the faster-reacting enantiomer in either the enzyme-substrate complex or the transition state (Fig. 3a). In the case of the non-lock-and-key mechanism, as found for the lipase- and subtilisin-catalyzed reactions, the slower-reacting enantiomer is destabilized by repulsive interactions and/or strains caused in the transition state, and even the faster-reacting enantiomer is not stabilized at all as compared to the reference substrate (Fig. 3b). Binding of the substrate to the enzyme is weak, as can be seen in Table 4. Despite weak binding, the subsequent reaction can be well accelerated by the great catalytic power of the enzyme, and a high degree of chiral discrimination can be achieved by a stereo-sensing mechanism operating in the transition state. It is well-known that some enzymes bind a substrate strongly to cause strains and/or to freeze out

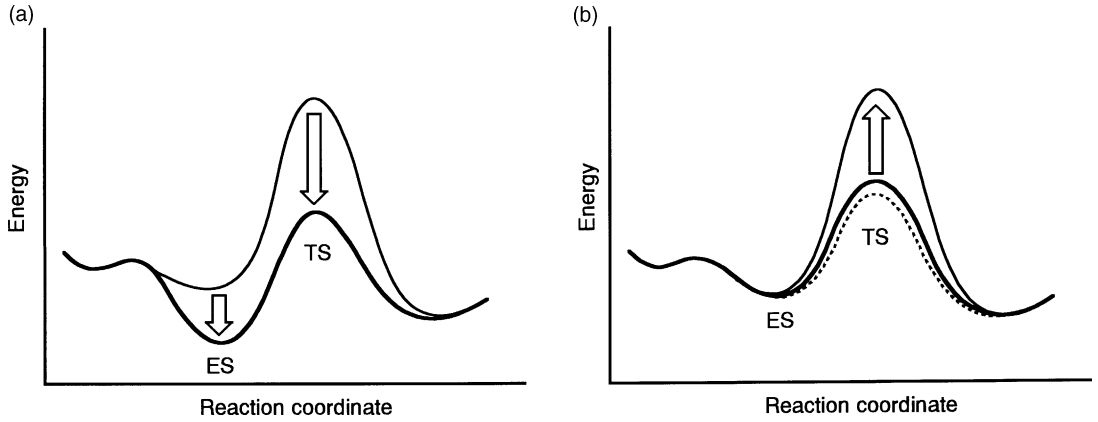

Fig. 3. Simplified energy diagrams representing (a) the lock-and-key mechanism and (b) the non-lock-and-key mechanism of enzyme-catalyzed kinetic resolutions. The energy diagram for the faster-reacting enantiomer is shown in a thick line, that for the slower-reacting enantiomer is in a thin line, and that for the reference substrate is in a broken line. ES and TS designate the enzyme-substrate complex and the transition state, respectively. (a) An extreme case of chiral discrimination based on the lock-and-key mechanism. The downward arrow represents the stabilization of the faster-reacting enantiomer due to binding interactions between enzyme's pockets and substrate's substituents. (b) Chiral discrimination based on the non-lock-and-key mechanism. The upward arrow represents the destabilization of the slower-reacting enantiomer due to repulsive interactions and/or strains caused in the transition state. Note that even the faster-reacting enantiomer is not stabilized at all as compared to the reference substrate. The lipase- and subtilisin-catalyzed kinetic resolutions of secondary alcohols can be represented by (b).

motions, promoting the subsequent reaction [67,68]. In such a case, tight binding with cooperative interactions is essential, which will however narrow substrate specificity. We consider that lipases and subtilisins, possessing the highly active catalytic residues (the catalytic triad and the oxyanion hole), can cleave/form the ester bond without causing strains and/or freezing out motions and that binding interactions between enzyme's pockets and substrate's substituents are therefore not essential for catalysis as well as enantioselectivity.

The non-lock-and-key concept can be consistent with both high stereoselectivity and broad substrate specificity if a stereo-sensing mechanism based on a definite chemical principle operates in the transition state. Because common sense that "enzymes have a great degree of specificity with respect to their substrates", found in textbooks [65], is being broken gradually by exhaustive studies in the field of biotransformation and biocatalysis, there may be other biocatalysts that can be classified into this new category. In other words, a biocatalyst of the non-lock-and-key type will be versatile and useful for organic synthesis.

4. Conclusions

It has long been believed that binding interactions between enzyme's pockets and substrate's substituents are essential for enantiomer discrimination. However, it is unlikely that lipases and subtilisins have binding pockets for discriminating the enantiomers of a variety of unnatural chiral compounds that have nothing to do with evolutionary pressure. Actually, there are no signs of preferential binding of the faster-reacting enantiomer in both the ground state and the transition state of the lipase- and subtilisin-catalyzed acylations of chiral secondary alcohols. Although the binding ability of these enzymes is poor in an organic solvent, the subsequent reaction is accelerated well by the great catalytic power of the enzymes which originates from the catalytic triad and the oxyanion hole, and a high degree of chiral discrimination is achieved by the stereo-sensing mechanism operating in the transition state. Enantioselectivity results from the suppression mechanism working on the slower-reacting enantiomer in the transition state. In an extreme case, the unfavorable enantiomer cannot pass over the transition state at all because of a very high activation energy

[50]. The “chemical reagent-like” feature (conformational requirements and repulsive interactions in the transition state) is predominant over the “enzymatic” feature (binding interactions at binding pockets). A new category of enzymatic reactions that is different from the traditional lock-and-key paradigm has been proposed for the enzymatic reactions toward unnatural substrates. Stereoselective enzymatic reactions can be classified into the following three types: (i) the lock-and-key type, (ii) the induced-fit type, and (iii) the non-lock-and-key type. The transition-state models are useful for explaining the behavior of the hydrolase-catalyzed enantioselective reactions toward unnatural substrates.

Acknowledgements

We are grateful to Amano Enzyme Inc. for providing us with lipase PS. We are also grateful to the SC-NMR Laboratory of Okayama University for the measurement of NMR spectra. This work was supported in part by a Grant-in-Aid for Scientific Research from the Ministry of Education, Science, Sports and Culture of Japan.

References

[1] C.-H. Wong, G.M. Whitesides, Enzymes in Synthetic Organic Chemistry, Elsevier, Oxford, 1994.
[2] K. Drauz, H. Waldmann (Eds.), Enzyme Catalysis in Organic Synthesis, vol. 1, VCH, New York, 1995.
[3] A.M.P. Koskinen, A.M. Klibanov (Eds.), Enzymatic Reactions in Organic Media, Blackie, Glasgow, 1996.
[4] U.T. Bornscheuer, R.J. Kazlauskas, Hydrolases in Organic Synthesis, Wiley/VCH, Weinheim, 1999.
[5] K. Faber, Biotransformations in Organic Chemistry, fourth ed., Springer, Berlin, 2000.
[6] H.-J. Gais, F. Theil, in: K. Drauz, H. Waldmann (Eds.), Enzyme Catalysis in Organic Synthesis, second ed., vol. 2, Wiley/VCH, Weinheim, 2002.
[7] Z.-F. Xie, I. Nakamura, H. Suemune, K. Sakai, J. Chem. Soc., Chem. Commun. (1988) 966.
[8] S.M. Roberts, Phil. Trans. R. Soc. Lond. B 324 (1989) 577.
[9] T. Umemura, H. Hirohara, in: J.R. Whitaker, P.E. Sonnet (Eds.), Biocatalysis in Agricultural Biotechnology, American Chemical Society, Washington, DC, 1989 (Chapter 26).
[10] R.J. Kazlauskas, A.N.E. Weissfloch, A.T. Rappaport, L.A. Cuccia, J. Org. Chem. 56 (1991) 2656.
[11] K. Burgess, L.D. Jennings, J. Am. Chem. Soc. 113 (1991) 6129.
[12] A.J.M. Janssen, A.J.H. Klunder, B. Zwanenburg, Tetrahedron 47 (1991) 7645.
[13] Z.-F. Xie, Tetrahedron: Asymmetry 2 (1991) 733.
[14] T. Itoh, K. Kuroda, M. Tomosada, Y. Takagi, J. Org. Chem. 56 (1991) 797.
[15] P.G. Hultin, J.B. Jones, Tetrahedron Lett. 33 (1992) 1399.
[16] K. Naemura, R. Fukuda, M. Murata, M. Konishi, K. Hirose, Y. Tobe, Tetrahedron: Asymmetry 6 (1995) 2385.
[17] U. Derewenda, A.M. Brzozowski, D.M. Lawson, Z.S. Derewenda, Biochemistry 31 (1992) 1532.
[18] M. Cygler, P. Grochulski, R.J. Kazlauskas, J.D. Schrag, F. Bouthillier, B. Rubin, A.N. Serreqi, A.K. Gupta, J. Am. Chem. Soc. 116 (1994) 3180.
[19] J. Uppenberg, M.T. Hansen, S. Patkar, T.A. Jones, Structure 2 (1994) 293.
[20] K.K. Kim, H.K. Song, D.H. Shin, K.Y. Hwang, S.W. Suh, Structure 5 (1997) 173.
[21] K. Lemke, M. Lemke, F. Theil, J. Org. Chem. 62 (1997) 6268.
[22] X. Grabuleda, C. Jaime, A. Guerrero, Tetrahedron: Asymmetry 8 (1997) 3675.
[23] F. Fæffner, T. Norin, K. Hult, Biophys. J. 74 (1998) 1251.
[24] C. Orrenius, F. Fæffner, D. Rotticci, N. Öhrner, T. Norin, K. Hult, Biocat. Biotrans. 16 (1998) 1.
[25] A.D. Cuiper, M.L.C.E. Kouwijzer, P.D.J. Grootenhuis, R.M. Kellogg, B.L. Feringa, J. Org. Chem. 64 (1999) 9529.
[26] A. Tafi, A. van Almsick, F. Corelli, M. Crusco, K.E. Laumen, M.P. Schneider, M. Botta, J. Org. Chem. 65 (2000) 3659.
[27] T. Schulz, J. Pleiss, R.D. Schmid, Protein Sci. 9 (2000) 1053.
[28] Y. Okahata, Y. Fujimoto, K. Ijiro, J. Org. Chem. 60 (1995) 2244.
[29] K. Nakamura, M. Kawasaki, A. Ohno, Bull. Chem. Soc. Jpn. 69 (1996) 1079.
[30] K. Nishizawa, Y. Ohgami, N. Matsuo, H. Kisida, H. Hirohara, J. Chem. Soc., Perkin Trans. 2 (1997) 1293.
[31] N. Kamiya, H. Kasagi, M. Inoue, K. Kusunoki, M. Goto, Biotechnol. Bioeng. 65 (1999) 227.
[32] P.L.A. Overbeeke, S.C. Orrenius, J.A. Jongejan, J.A. Duine, Chem. Phys. Lipids 93 (1998) 81.
[33] P.L.A. Overbeeke, C. Govardhan, N. Khalaf, J.A. Jongejan, J.J. Heijnen, J. Mol. Catal. B: Enzymatic 10 (2000) 385.
[34] P.L.A. Overbeeke, J.A. Jongejan, J.J. Heijnen, Biotechnol. Bioeng. 70 (2000) 278.
[35] Y. Hirose, K. Kariya, Y. Nakanishi, Y. Kurono, K. Achiwa, Tetrahedron Lett. 36 (1995) 1063.
[36] M.T. Reetz, A. Zonta, K. Schimossek, K. Liebeton, K.-E. Jaeger, Angew. Chem. Int. Ed. Engl. 36 (1997) 2830.
[37] H. Scheib, J. Pleiss, P. Stadler, A. Kovac, A.P. Potthoff, L. Haalck, F. Spener, F. Paltauf, R.D. Schmid, Protein Eng. 11 (1998) 675.
[38] N.A. Turner, D.J.H. Gaskin, A.T. Yagnik, J.A. Littlechild, E.N. Vulfson, Protein Eng. 14 (2001) 269.
[39] D. Rotticci, J.C. Rotticci-Mulder, S. Denman, T. Norin, K. Hult, ChemBioChem 2 (2001) 766.
[40] M.T. Reetz, S. Wilensek, D. Zha, K.-E. Jaeger, Angew. Chem. Int. Ed. 40 (2001) 3589.
[41] R. Utsumi, S. Izumi, T. Hirata, Chem. Lett. (2001) 892.

[42] T. Ema, J. Kobayashi, S. Maeno, T. Sakai, M. Utaka, Bull. Chem. Soc. Jpn. 71 (1998) 443.
[43] R.E. Gawley, J. Aubé, Principles of Asymmetric Synthesis, Elsevier, Oxford, 1996.
[44] T. Ema, R. Okada, M. Fukumoto, M. Jittani, M. Ishida, K. Furuie, K. Yamaguchi, T. Sakai, M. Utaka, Tetrahedron Lett. 40 (1999) 4367.
[45] P.A. Fitzpatrick, A.M. Klibanov, J. Am. Chem. Soc. 113 (1991) 3166.
[46] R.J. Kazlauskas, A.N.E. Weissfloch, J. Mol. Catal. B: Enzymatic 3 (1997) 65.
[47] R.C. Lloyd, M. Dickman, J.B. Jones, Tetrahedron: Asymmetry 9 (1998) 551.
[48] T. Ema, K. Yamaguchi, Y. Wakasa, N. Tanaka, M. Utaka, T. Sakai, Chem. Lett. (2000) 782.
[49] T. Ema, M. Jittani, T. Sakai, M. Utaka, Tetrahedron Lett. 39 (1998) 6311.
[50] T. Ema, M. Jittani, K. Furuie, M. Utaka, T. Sakai, J. Org. Chem. 67 (2002) 2144.
[51] C.-S. Chen, Y. Fujimoto, G. Girdaukas, C.J. Sih, J. Am. Chem. Soc. 104 (1982) 7294.
[52] Z.S. Derewenda, Y. Wei, J. Am. Chem. Soc. 117 (1995) 2104.
[53] D.J. Neidhart, G.A. Petsko, Protein Eng. 2 (1988) 271.
[54] C.A. McPhalen, M.N.G. James, Biochemistry 27 (1988) 6582.
[55] I. Schechter, A. Berger, Biochem. Biophys. Res. Commun. 27 (1967) 157.
[56] A. Fersht, Enzyme Structure and Mechanism, second ed., Freeman, New York, 1985 (Chapter 3).
[57] J.N. Israelachvili, Intermolecular and Surface Forces, Academic Press, London, 1985.
[58] R.S. Phillips, Trends Biotechnol. 14 (1996) 13.
[59] T. Sakai, I. Kawabata, T. Kishimoto, T. Ema, M. Utaka, J. Org. Chem. 62 (1997) 4906.
[60] T. Sakai, T. Kishimoto, Y. Tanaka, T. Ema, M. Utaka, Tetrahedron Lett. 39 (1998) 7881.
[61] K. Naemura, K. Matsunaga, J. Fuji, K. Ogasahara, Y. Nishikawa, K. Hirose, Y. Tobe, Anal. Sci. 14 (1998) 175.
[62] R. Hoffmann, Y. Inoue, J. Am. Chem. Soc. 121 (1999) 10702.
[63] N.A. Turner, E.C. Needs, J.A. Khan, E.N. Vulfson, Biotechnol. Bioeng. 72 (2001) 108.
[64] E. Fischer, Ber. Dt. Chem. Ges. 27 (1894) 2985.
[65] D. Voet, J.G. Voet, Biochemistry, second ed., Wiley, New York, 1995.
[66] D.E. Koshland Jr., Proc. Natl. Acad. Sci. U.S.A. 44 (1958) 98.
[67] R. Wolfenden, M.J. Snider, Acc. Chem. Res. 34 (2001) 938.
[68] T.C. Bruice, Acc. Chem. Res. 35 (2002) 139.